Football Video Image Restoration Based on Generalized Equalized Fuzzy C-mean Clustering Algorithm

Shaonan Liu
Songshan Shaolin Wushu College, Dengfeng, 452470, China

***Abstract*—With the development of image processing techniques, the quality of visual content has become crucial for acquiring and analyzing information, especially in applications in the field of sports, such as football match videos. Conventional image restoration techniques have limitations in dealing with motion blur and noise interference, especially in maintaining edge information and texture details. Aiming at these challenges, the study presents a generalized balanced fuzzy C-mean clustering algorithm incorporating fuzzy logic and cluster analysis by introducing local spatial information and adaptive edge protection factors, and the generalized balanced fuzzy C-mean clustering algorithm optimizes the updating strategies of the affiliation function and the class center in order to enhance the detail preservation and noise suppression, aiming to improve the recovery quality of football video images. The results demonstrated that the average gradient ratio, edge strength, standard deviation, and information entropy of the designed algorithm were 1.77, 0.92, 0.26, and 1.73, respectively, which were significantly better than those of other algorithms, proving its superiority in image restoration. Football video images can be made clearer and more detailed with the help of the generalized balanced fuzzy C-mean clustering technique, which also advances motion analysis and automatic identification technologies.**

***Keywords*—Generalized equilibrium; fuzzy c-mean clustering algorithm; image restoration; local spatial information; adaptive edge protection factor**

I. Introduction

A. Background Introduction

The gathering and examination of visual content has grown in popularity as multimedia and image-processing technologies have advanced. Especially in the field of sports, video images, as an important information transfer medium, provide rich visual materials for game analysis, athlete performance evaluation and spectator experience [1-2]. However, due to the limitation of shooting conditions and interference during transmission, football video images (FVIs) often suffer from blurring and noise interference, which adversely affects the quality of the images and subsequent analysis. Therefore, quality restoration of FVI is not only important for enhancing the viewing experience of viewers, but also for professional analysts to conduct technical analysis. Image restoration (IR) technique aims to recover clear images from damaged or degraded images, this technology can effectively remove noise, blur, and distortion from images, thereby improving the quality and clarity of the images [3-4].

B. Current Research Challenges

Although traditional restoration techniques have made some progress, the complexity of the scene dynamics, the fast movement of athletes and balls, and the change of ambient lighting make IR more challenging when dealing with FVI [5-6]. In addition, the unclear boundaries of different objects in FVI, as well as the unclear separation of background and foreground, are problems that need to be solved with more refined and efficient algorithms. Because of this, it is very important to create a restoration algorithm that can handle the issues unique to FVI. The algorithm needs to accommodate motion blurring (MB) and noise interference in the image while maintaining the integrity of image details for subsequent image analysis and information extraction.

C. Proposed Methods

The research aims to develop an efficient and accurate image restoration algorithm to improve the quality and clarity of football video images [7]. Therefore, the study designs an IR method based on generalized equilibrium fuzzy C-means clustering (GECM) algorithm. The method segments the image by introducing a fuzzy clustering algorithm and then restores the image in the framework of fuzzy sets.

D. Innovation and Contribution

The innovation of this study is that the algorithm combines the advantages of fuzzy logic and cluster analysis, as well as the ideas of generalized equilibrium theory, which not only improves the accuracy of IR, but also enhances the robustness of the algorithm in dealing with fuzzy and uncertain information. The contribution of this study is to provide a new technical approach for IR of football video (FV). It is crucial in advancing later applications like motion analysis and automatic recognition in addition to improving the viewing experience of FV.

E. Organization Structure

The research is divided into six sections. Section I is a background introduction of IR for FVs technology. Section II is a review of the current research status of IR technology for FV at home and abroad. Section III is the implementation process of GECM algorithm designed on the basis of fuzzy C-means (FCM) clustering algorithm. Section IV is the performance analysis of GECM algorithm and its effect analysis in practical applications. Discussion is given in Section V. Section VI is a summary of the whole paper and points out the shortcomings.

II. Related Works

With the wide application of FV, there is an increasing demand for IR of FV. However, FVI often suffers from blurring and distortion due to the limitation of the shooting environment and the noise during video transmission. To address this problem, scholars have proposed a series of IR techniques. Zhang and other researchers designed a deep convolutional neural network-based noise reduction prior to solve the problem of plug-and-play IR. The results revealed that the method has a better recovery effect [8]. A generative adversarial model for IR based on physics was created by Pan and other researchers to address the undefined problems of image deblurring, image defogging, and image deblurring. The model is trained end-to-end and provides guidance for the estimation process for a given task inside the generative adversarial network. The results revealed that the model outperforms the existing algorithms [9]. Zha et al. designed an IR method based on a hybrid structured sparse error model in response to the problem of overfitting the internal model in traditional methods, which was applied to the tasks of IR, image compression perception, and image cloud blocking using an alternating minimization algorithm. The results indicated that the method was more effective in terms of objective metrics and visual perception [10]. Mei et al. created a pyramid attention module that can remove signals at coarser levels and captures long-range feature correspondences from a multi-scale feature pyramid in order to address the issue of underutilizing self-similarity in deep convolutional neural network IR methods. The results showed better accuracy and visual quality of the method based on this module [11]. In order to address the issue of increased runtime in hyperspectral infrared imaging, He researchers created a unified paradigm that combines spatial and spectral attributes for the recovery method. This paradigm takes advantage of the performance benefits of non-local spatial denoising and low computational complexity of low-rank orthogonal basis exploration. The approach performs better than current methods, according to the results [12].

Hu and colleagues developed a ranking learning framework based on pairwise comparisons to objectively assess the performance of IR algorithms. This framework integrates quality-aware features in both the air and frequency domains and introduces a generalized IR quality metric. The framework performs well in terms of generalization, according to the findings [13]. Jiu and other researchers designed a deep primal-pairwise proximity network in order to solve the more time-consuming problem of optimizing the log-likelihood function for minimizing non-smooth penalties in IR, which reformulates the primal-pairwise hybrid gradient algorithm as a deep network with fixed layers. The results revealed that this method has a better image recovery effect [14]. Chen et al. designed a group sparse regularization method for spatially differenced images for the presence of mixed noise in hyperspectral images. The outcomes proved how effective this strategy is at recovering hyperspectral images [15]. Yu and other scholars designed a multi-path convolutional neural network called Path-Restore for the problem of excessive computational burden of deep convolutional neural network in IR task. The results revealed the low computational cost of this method [16]. Zamir and other researchers designed a new method MIRNet-v2 in order to solve the problems in convolutional neural network based methods, which maintains a high resolution representation through multi-scale feature extraction and information exchange. Additionally, the outcomes demonstrate this method's superiority across various datasets [17].

In summary, scholars have proposed many methods to improve the recovery effect and performance in the field of IR, and significant progress has been made. However, these methods still have some shortcomings in terms of running time and computational burden. Thus, in order to enhance the visual quality of FV, the study presents adaptive edge protection factor (AEPF) and local spatial information and creates a GECM method based on the conventional FCM technique.

III. Image Restoration Technique for Football Video based on GECM Algorithm

This chapter focuses on the design process of GECM algorithm, the first section is the design of IR technique for FV based on traditional FCM algorithm, and the second section is the design of GECM algorithm with improvement in traditional FCM algorithm.

A. Image Restoration Technique for Football Video Based on FCM Algorithm

In IR of complex dynamic scenes such as FV, traditional restoration techniques often perform poorly in dealing with blurred boundaries and MBs in the face of dynamic and complex scenes as well as fast-moving athletes and footballs [18-19]. These techniques often ignore the uncertainty and blurring information in the image when recovering a clear image, resulting in the inability to appropriately preserve the detailed features in a dynamic scene. To address this issue, the study proposes an IR technique for FV using the FCM algorithm. The FCM algorithm allows for adaptable grouping of image pixels by introducing the concept of degree of affiliation. It allows pixels to belong to multiple clusters with different degrees of affiliation, dividing the pixels in an image into multiple distinct subsets, each corresponding to a specific image feature, thus aiding in noise removal and image quality improvement [20-21]. The weighted sum of the distances between the data points and the cluster centers is quantified by an objective function (OF) that is defined at the core of the FCM clustering algorithm. To achieve soft clustering of the pixels, this function is iteratively refined. The expression of the OF for FCM is shown in Eq. (1).

$$J(U,V)=\sum_{i=1}^{N}\sum_{j=1}^{C}u_{ij}^{m}d^{2}(x_i,v_j) \tag{1}$$

In Eq. (1), N is the total number of data points being clustered, i.e., the total pixels in the image. C represents the clustering centers (CCs), and u_{ij} is the degree of affiliation of the i th data point belonging to the j th CC. m represents the fuzzy parameter, which is a constant greater than 1 and is usually set to 2 to adjust the fuzziness of the affiliation. d represents the Euclidean distance and x_i is the pixel value of the i th data point. v_j represents the pixel value of the j th CC. The FCM clustering schematic is shown in Fig. 1.

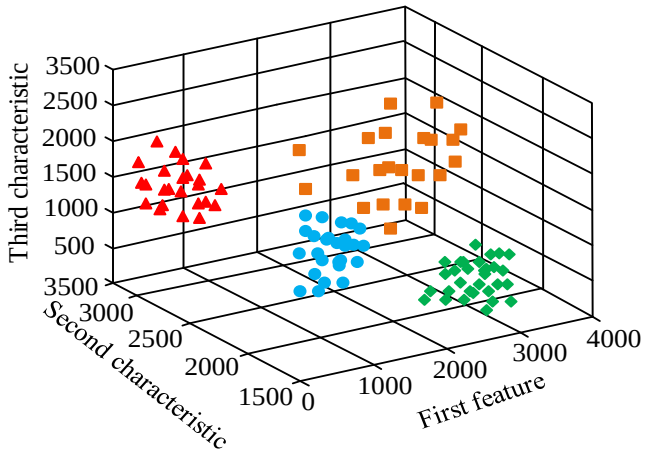

Fig. 1. FCM clustering diagram.

The FCM clustering algorithm optimizes the affiliation function and CCs iteratively so that pixels in the same region are clustered together. This allows the IR process to deal with different regions in more detail, especially in the case of blurred boundaries. To minimize the effect of noise on the recovery process, the study smoothes the image by applying a Gaussian filter to reduce the noise and, at the same time, maintains the edge information with the expression shown in Eq. (2).

$$H(x,y)=\frac{1}{2\pi\sigma^2}e^{(-\frac{x^2+y^2}{2\sigma^2})} \tag{2}$$

In Eq. (2), $H(x,y)$ represents the two-dimensional Gaussian function, x,y represents the pixel position, and σ represents the standard deviation (SD) of the Gaussian distribution. The affiliation matrix can reflect the affiliation of the pixel with the CC, the affiliation matrix, and the CC need to be initialized at the beginning of the clustering, and the CC initialization method is shown in Eq. (3).

$$D(x)=\min_{1\le i\le k}\left\|x-v_i\right\|^2 \tag{3}$$

In Eq. (3), represents the distance between data point x and the nearest CC i. The new CC is chosen based on which data point is the furthest from the existing CC in order to enhance the clustering quality and accelerate the algorithm's convergence. Either uniform or random assignment can be used to determine the affiliation matrix's starting value. Equation (4) is utilized to initialize the attachment degree (AD) and guarantee that its total equals 1.

$$u_{ij}^0=\frac{1}{C}\quad \forall i,j \tag{4}$$

In Eq. (4), u_{ij}^0 represents the initial affiliation of pixel i to the CC j. The next step is to update the affiliation with the CC using the minimization OF, and the expression of the minimization OF is shown in Eq. (5).

$$\min\left\{J_m(U,V)\right\}=\sum_{i=1}^{N}\min\left\{\sum_{i=1}^{C}u_{ij}^m\left\|x_i-v_j\right\|^2\right\} \tag{5}$$

In Eq. (5), $\min(\cdot)$ stands for minimization. The affiliation and CC update rules are shown in Eq. (6).

$$\begin{cases} u_{ij}=\dfrac{1}{\sum_{k=1}^{C}(\frac{d_{ij}^2}{d_{ij}^2})^{\frac{1}{m-1}}} \\ v_j=\dfrac{\sum_{j=1}^{N}u_{ij}^m x_i}{\sum_{j=1}^{N}u_{ij}^m} \end{cases} \tag{6}$$

In Eq. (6), m represents the CCs and k represents the CC index. The updating process continues until the change of affiliation and CC is below a certain threshold, i.e., the iteration reaches convergence, thus ensuring the optimal classification of pixel points. During the IR process, differentiated processing strategies can be used for different feature regions, such as maintaining details in textured regions and enhancing smoothing in uniform regions, namely denoising. After obtaining the segmentation results, the affiliation of each pixel is regarded as a parameter of the denoising process, and the denoising of the pixel points is performed by weighted average. Then the computation of the pixel value after denoising is shown in Eq. (7).

$$y_i=\frac{\sum_{j\in N_i}u_{ij}^m x_j}{\sum_{j\in N_i}u_{ij}^m} \tag{7}$$

In Eq. (4), represents the pixel value after denoising process and N_i represents the set of pixel points adjacent to pixel point i. Noise suppression within a local area is achieved by assigning a degree of affiliation to each pixel point and using this degree of affiliation as used as a weighting factor, combined with the values of neighboring pixel points. The FCM clustering process is shown in Fig. 2.

To ensure that the edge information is not over-smoothed in the denoising process, the study introduces the Sobel edge detection operator. This factor combines the pixel gray level differences within a local neighborhood to identify the edge strength in the image. Using the edge protection factor, the intensity of each pixel denoising can be adjusted to maintain the sharpness and detail of the edges [22-23]. The horizontal and vertical convolution kernel expressions for the Sobel operator are shown in Eq. (8).

$$\begin{cases} G_x = \begin{bmatrix} -1 & 0 & 1 \\ -2 & 0 & 2 \\ -1 & 0 & 1 \end{bmatrix} * A \\ G_y = \begin{bmatrix} -1 & -2 & -1 \\ 0 & 0 & 0 \\ 1 & 2 & 1 \end{bmatrix} * A \end{cases} \quad (8)$$

In Eq. (8), G_x represents the horizontal image gradient, G_y represents the vertical image gradient, and A represents the image matrix. So far, the design of IR technique is completed and the IR process is shown in Fig. 3.

B. GECM Algorithm Design

The need for detail preservation and noise suppression is especially critical for IR techniques when dealing with blur and noise problems in video images. FVI, due to its complex dynamics and the limitations of traditional FCM in terms of AD updating and class center definition, is not fine enough to deal with MB and background noise, especially in maintaining edge information and texture details [24-25]. Therefore, the study designs an IR method based on the GECM algorithm by introducing new optimization mechanisms and constraints, improving the updating strategies of the example degree function and class centers, and enhancing the detail preservation and noise suppression in the IR process. Firstly, the FCM algorithm is improved by introducing local spatial information as a priori, and a generalized OF considering pixel spatial neighborhood information is constructed, the expression of which is shown in Eq. (9).

$$J_{GECM} = \sum_{i=1}^{N} \sum_{j=1}^{C} u_{ij}^{m} \left(\left\| x_i - v_j \right\|^2 + \alpha \sum_{k \in N_i} w_{ik} \left\| x_i - x_k \right\|^2 \right) \quad (9)$$

In Eq. (9), α represents the regularization parameter, which can determine the influence of spatial information, and w_{ik} represents the similarity weight between pixel i and its neighboring pixel k, which can reflect the closeness of spatial location. This OF not only considers the Euclidean distance from the data point to the CC, but also integrates the similarity between the pixel point and its spatial domain. By adding the last term, the spatial continuity within the class can be enhanced, thus better preserving the local structural properties of the image. The spatial weights are calculated as shown in Eq. (10).

$$w_{ik} = e^{\left(-\frac{\left\| p_i - p_k \right\|^2}{2\delta^2}\right)} \quad (10)$$

In Eq. (10), p_i represents the position coordinates of pixel i, p_k represents the position coordinates of pixel k, and δ represents the parameter controlling the influence range of spatial weights. The next step is to adjust the updating rules of the AD and CC to fit the generalized OF and reflect the influence of the neighborhood information. The adjusted affiliation update rule is shown in Eq. (11).

$$u'_{ij} = \left(\frac{\frac{1}{\left\| x_i - v_j \right\|^2 + \alpha \sum_{k \in N_i} w_{ik} \left\| x_i - x_k \right\|^2}}{\sum_{k=1}^{C} \frac{1}{\left\| x_i - v_k \right\|^2 + \alpha \sum_{k \in N_i} w_{il} \left\| x_i - x_l \right\|^2}} \right)^{\frac{1}{m-1}} \quad (11)$$

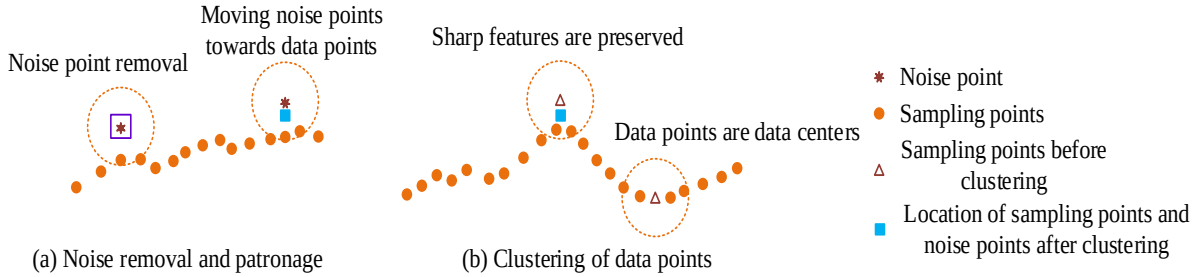

Fig. 2. FCM clustering process.

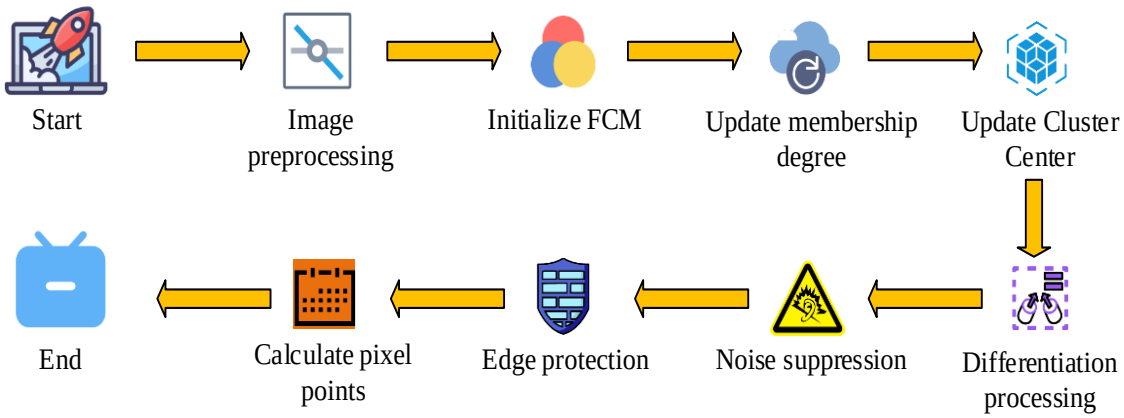

Fig. 3. Image restoration process based on FCM algorithm.

In Eq. (11), represents the adjusted AD and w_{il} represents the similarity weight between pixel i and its neighbor pixel l. The update rule for the adjusted CC is shown in Eq. (12).

$$v_j' = \frac{\sum_{i=1}^{N} u_{ij}^m x_i + \alpha \sum_{i=1}^{N} \sum_{k \in N_i} w_{ik} u_{ij}^m x_k}{\sum_{i=1}^{N} u_{ij}^m + \alpha \sum_{i=1}^{N} \sum_{k \in N_i} w_{ik} u_{ij}^m} \tag{12}$$

In Eq. (12), v_j' represents the adjusted CC. To enhance the algorithm's capacity to suppress noise, the research adds the AEPF, whose expression is represented by Eq. (13), to modify the degree of edge protection during the clustering update process.

$$\beta_{ij} = e^{-\gamma |\nabla x_i|} \tag{13}$$

In Eq. (13), β_{ij} represents AEPF and γ represents the parameter that controls the edge protection strength. AEPF combined with Sobel edge detection results can correct the updating formula of the CC, and the improved CC updating formula is shown in Eq. (14).

$$v_j = \frac{\sum_i^N u_{ij}^m \beta_{ij} x_i}{\sum_i^N u_{ij}^m \beta_{ij}} \tag{14}$$

This correction allows the algorithm to take more account of edge protection when updating the CCs, reducing blurring and loss of detail in the edge regions. Finally, the image is recovered using the updated AD and CCs, and during the recovery process, the new value of each pixel is determined by its AD-weighted CC value, which is calculated as shown in Eq. (15).

$$x_i' = \sum_{j=1}^{C} u_{ij} v_j \tag{15}$$

In Eq. (15), x_i' represents the new value of pixel i after recovery. Finally, the restoration effect is further enhanced by the denoising algorithm with non-local averaging, and the final pixel points are calculated as shown in Equation (16).

$$x_i'' = \frac{1}{Z_i} \sum_{k \in N_i} e^{\left(-\frac{\|x_i' - x_k'\|^2}{h^2}\right) x_k'} \tag{16}$$

In Eq. (16), x'' represents the final recovered value of pixel i, Z_i represents the normalization factor, and h represents the smoothing parameter, which controls the sensitivity of the similarity weights in the nonlocal mean denoising algorithm. The GECM algorithm flow is shown in Fig. 4.

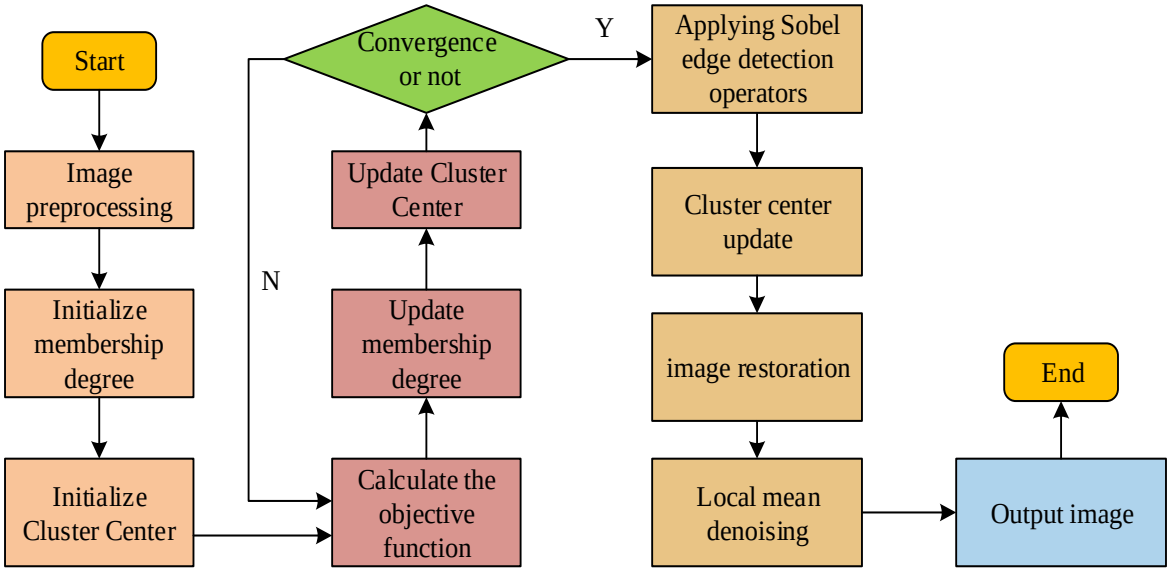

Fig. 4. Image restoration process based on FCM algorithm.

IV. Results

This chapter concentrates on the GECM algorithm's experimental findings in the IR of FV. The GECM algorithm's performance analysis is presented in the first section, and its effect analysis in real-world applications is shown in the second.

A. Performance Analysis of the GECM Algorithm

The study chooses 300 picture samples from the ImageNet dataset for experimentation in order to confirm the effectiveness of the developed GECM method. Table I displays the relevant parameter settings.

Firstly, the samples are clustered using the GECM algorithm and the FCM algorithm respectively, set the category of clustering as 2, the maximum iterations is 100, and 10 experiments are carried out, and the distribution of the sample space after clustering by different algorithms is shown in Fig. 5.

TABLE I. EXPERIMENTAL RELATED PARAMETERS

Category	Parameter/ Specification	Description	Value/Details
Algorithm Parameter	Iterations	Number of complete training cycles	100
	batch size	Number of samples used during each training session	32
	Learning rate	Control the step size of parameter updates	0.01
Hardware Specification	CPU	The operation and control core of computers	2.6GHz Intel Core i7-7700
	RAM	Temporary storage devices for computers	16GB

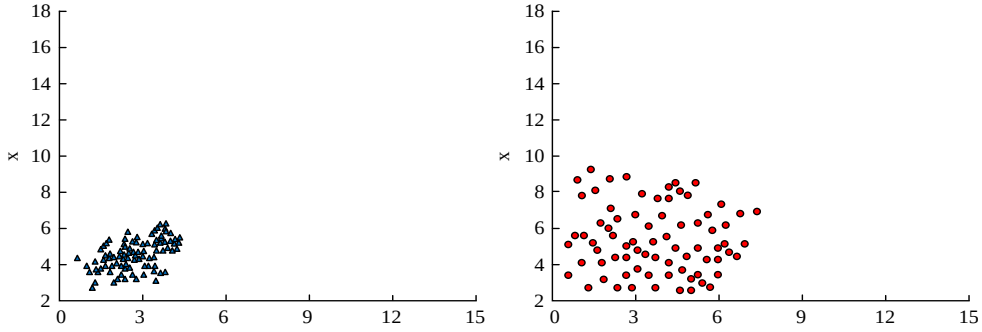

Fig. 5. Sample spatial distribution after clustering using different algorithms.

In Fig. 5(a), the samples are clustered by the GECM algorithm, and the samples show a denser spatial distribution. It shows that the GECM algorithm can effectively cluster similar image samples together and form dense clusters. Fig. 5(b) shows the spatial distribution of the FCM algorithm after clustering the same image samples. Compared with GECM, the clustering results of the FCM algorithm show a more decentralized spatial distribution. The above results illustrate that the GECM algorithm shows better performance in image sample clustering, captures the similarity between image samples better, and provides more accurate IR results. In the next step, on the ImageNet dataset, the AD curves of different algorithms under different CCs are calculated separately and compared with the ideal curves, and the results are shown in Fig. 6.

In Fig. 6(a), when the CC is 0, the AD curve of the designed GECM algorithm is closer to the ideal curve, while the AD curve of the FCM algorithm is slightly off. This indicates that in this case, the GECM algorithm is closer to the ideal state than the FCM algorithm in calculating the AD, which more accurately portrays the degree of belonging of the data points to the CC. In Fig. 6(b), the AD curve of the GECM algorithm is also closer to the ideal curve when the CC is 2. In summary, the GECM algorithm exhibits an AD curve closer to the ideal curve, whether the CC is 0 or 1. The GECM algorithm can improve the quality and accuracy of clustering results. Finally, 1 group of samples in ImageNet dataset and FIFA World Cup dataset is selected to calculate the running time of GECM algorithm and compare it with FCM algorithm and Bilateral Filtering (BF). Additionally, Fig. 7 displays the comparison results.

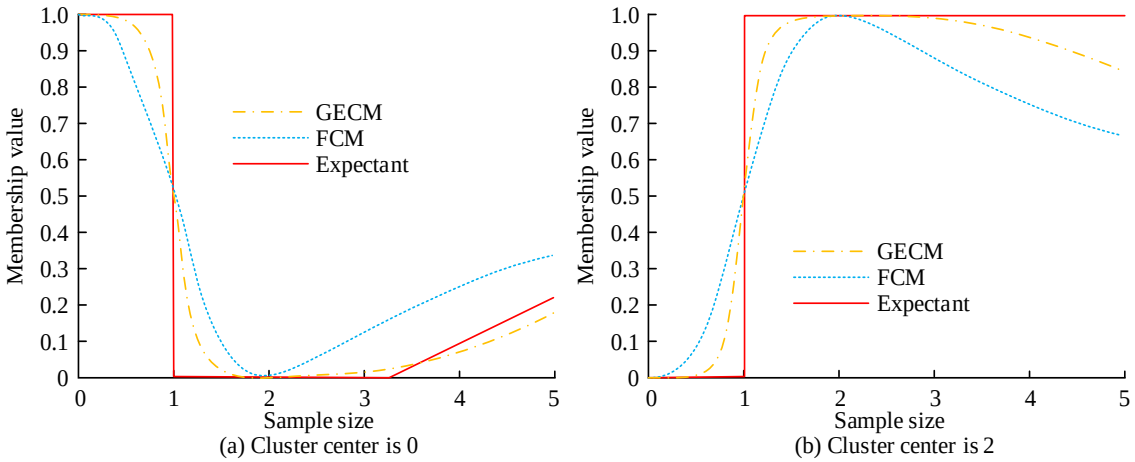

Fig. 6. Membership curves of different algorithms under different clustering centers.

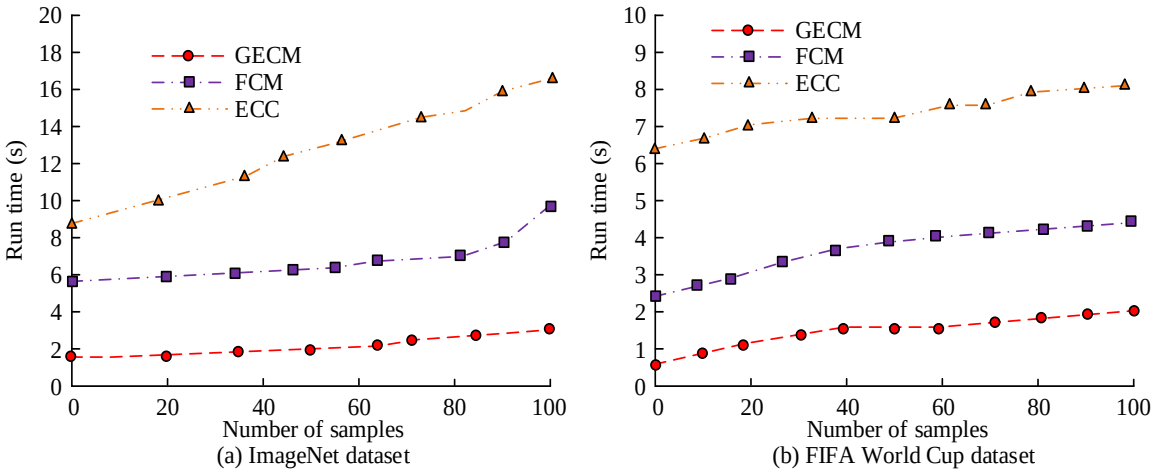

Fig. 7. The running time of different algorithms.

In Fig. 7(a), in the ImageNet dataset, the average running time of the designed GECM algorithm is 2.45s, that of the FCM algorithm is 7.73s, and that of the BF algorithm is 12.41s. In Fig. 7(b), in the FIFA World Cup dataset, the average running time of the three algorithms are 1.26s, 3.45s, and 7.24s. The above results illustrate that the GECM algorithm shows faster running speed on different datasets, and it is able to process FVI faster and with higher efficiency compared to the FCM algorithm and the BF algorithm.

B. Effect of Practical Application of GECM Algorithm

To verify the practical application effect of the designed GECM algorithm, the processor studied is 2.6GHz Intel Core i7-7700, running with 16GB of RAM, under Windows 10 operating system, and simulation experiments are conducted using Matlab R2018a. Firstly, four parameters, namely mean gradient ratio, edge strength, SD and information entropy are introduced to evaluate the IR effect of the GECM algorithm and compared with the FCM algorithm, BF algorithm, and median filtering (MF) algorithm. And Table II displays the outcomes.

In Table II, the average gradient ratio, edge strength, SD, and information entropy of the designed GECM algorithm are 1.77, 0.92, 0.26, and 1.73, respectively. The average gradient ratio increased by 20.41% compared to the lowest value of 1.47, the edge strength increased by 10.84% compared to the lowest value of 0.83, and the SD as well as the information entropy increased by 23.81% and 8.80% respectively compared to the lowest values of the two metrics values. The above results illustrate the ability to better preserve image details and edge information, increase image details and textures, as well as preserve complex texture and detail information. It proves the superiority of GECM algorithm in IR. The next step is to calculate the image edge information loss rate under different algorithms and compare it with the actual image edge information loss rate to verify the accuracy and fidelity of IR and the results are shown in Fig. 8.

TABLE II. AVERAGE GRADIENT RATIO, EDGE STRENGTH, STANDARD DEVIATION, AND INFORMATION ENTROPY OF DIFFERENT ALGORITHMS

Algorithm	Average gradient ratio	Edge strength	Standard deviation	Information entropy
MF	1.47	0.86	0.23	1.59
BF	1.53	0.83	0.24	1.61
FCM	1.62	0.87	0.21	1.67
GECM	1.77	0.92	0.26	1.73

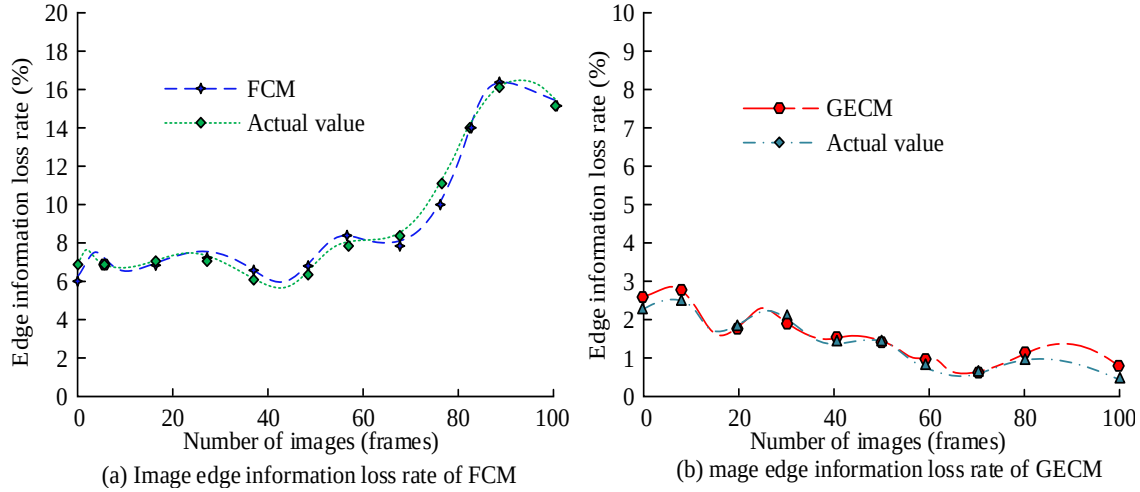

Fig. 8. The loss rate of image edge information under different algorithms.

The FCM algorithm's image edge information loss rate is shown to increase steadily in Fig. 8(a) as the number of images increases, however there are discrepancies between the algorithm's estimate and the actual image edge information loss rate. The picture edge information loss rate of the GECM algorithm is shown in Fig. 8(b) to gradually decrease as the number of images increases. And at the same time, there is basically no error between it and the actual image edge information loss rate. This indicates that the GECM algorithm performs better in retaining image edge information with higher accuracy and fidelity. In the next step, two indexes, peak signal-to-noise ratio and structural similarity, are introduced, and Cameraman, Barbara, and Pepper from the standard graphic library are used as test images to calculate the index values of different algorithms to further verify the IR effect of the designed algorithms, and the results are shown in Table III.

In Table III, the peak SNR and structural similarity of the GECM algorithm are 28.23 and 0.915 for the Cameraman test image, 29.26 and 0.943 for the Barbara test image, and 30.67 and 0.944 for the Pepper test image. It can be found that for all three test images, the GECM algorithm has the highest peak SNR and structural similarity, indicating that it can better maintain the signal quality and structural similarity of the images. 30.67, 0.944. It can be concluded that for all the three test images, the peak SNR and structural similarity of the GECM algorithm are the highest, indicating that it is able to better maintain the signal quality and structural similarity of the images. Finally, the study restores a set of real FVIs by different algorithms to verify the practical effect of the designed algorithms, and the results are shown in Fig. 9.

TABLE III. PEAK SIGNAL-TO-NOISE RATIO AND STRUCTURAL SIMILARITY OF DIFFERENT ALGORITHMS

Algorithm	Cameraman		Barbara		Pepper	
	PSNR	***SSIM***	***PSNR***	***PSNR***	***SSIM***	***SSIM***
MF	23.37	0.776	24.86	0.814	27.74	0.898
BF	25.39	0.854	26.75	0.847	28.01	0.903
FCM	25.98	0.872	28.61	0.902	29.51	0.917
GECM	28.23	0.915	29.26	0.943	30.67	0.944

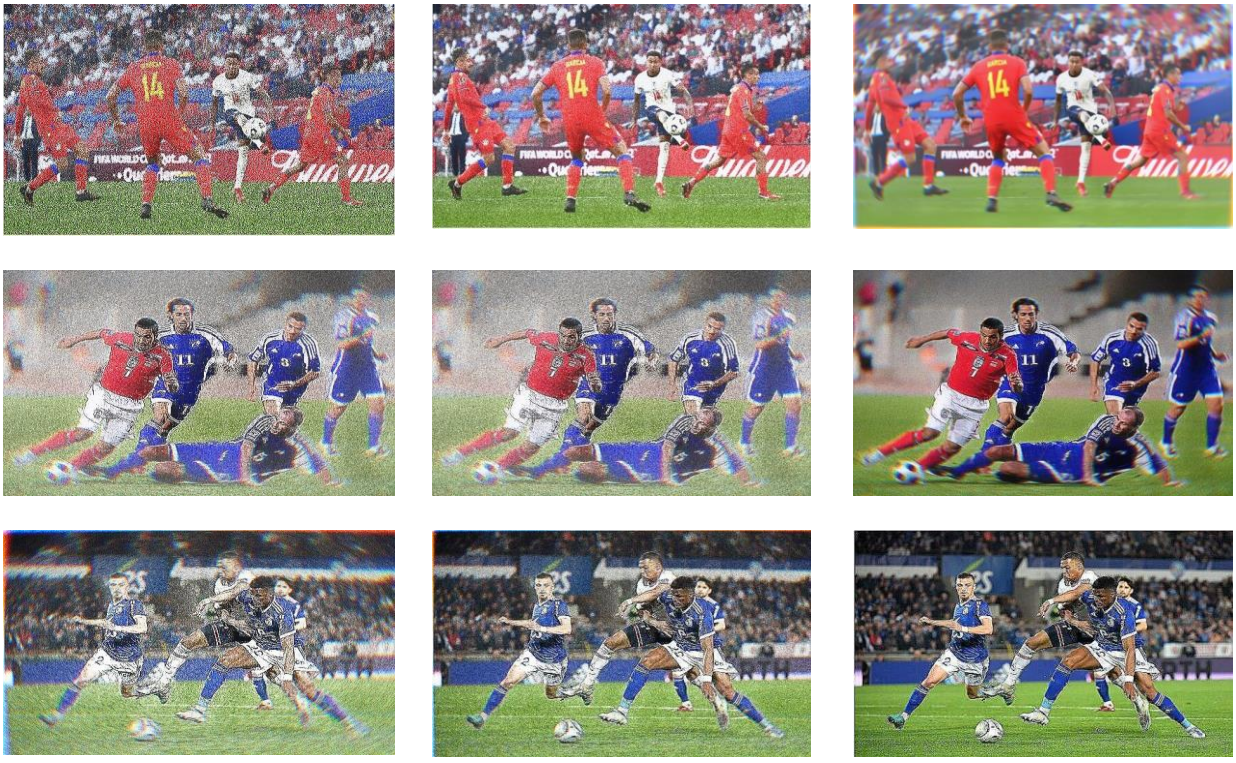

(a) Original (b) FCM (c) GECM

Fig. 9. Comparison of actual image restoration effects.

Fig. 9 (a) shows the original image, Fig. 9 (b) shows the image after restoration processing using the FCM algorithm, and Fig. 9 (c) shows the image after restoration processing using the GECM algorithm. From Fig. 9, the image recovered by the GECM algorithm has a far greater level of clarity than both the original and the FCM-processed images. It can be seen that the clarity and details of the original image have been restored, and the recovered image has some improvement over it. It demonstrates that it works better in IR.

V. DISCUSSION

This study focuses on the noise and blur problems in football video images. Based on the generalized equilibrium theory, the FCM algorithm is optimized and a new GECM algorithm is designed to restore the clarity and details of blurred images. The experimental results show that when trained on the ImageNet dataset and FIFA World Cup dataset, the performance of the GECM algorithm is superior to other algorithms. This is

consistent with the conclusion drawn by Neole [26]. The model proposed by Neole maintains high robustness on different datasets. This is because the GECM algorithm introduces the generalized equilibrium theory, which enables it to better adapt to various complex image content and noise situations when processing different types of image data. The average runtime of the proposed GECM algorithm on different datasets is 1.26s and 2.45s, respectively. Chen et al [27]. proposed a lightweight image restoration method based on group convolution and attention mechanism, and the results showed that this method ensures the quality of image restoration while significantly reducing the time required for image restoration compared to other methods. This method obtained consistent results with this article. However, this method has not been tested on different datasets, and its universality is still insufficient. Compared with it, the algorithm in this paper is significantly better. Compared with the sub-pixel reconstruction method based on deep learning proposed by Li et al. [28], the PSNR of this paper can reach up to 30.67, and the SSIM can reach up to 0.943. In terms of maintaining the signal quality and structural similarity of the image, this method is significantly better. This may be because the GECM algorithm introduces an adaptive edge protection factor, which can ensure the clarity of the edges and the texture details of the image during the image restoration process, thereby improving the PSNR and SSIM values. In summary, the GECM algorithm is a novel image restoration technique that can significantly improve the accuracy and efficiency of image restoration.

VI. Conclusion

In the context of the rapid development of modern multimedia technology and image processing technology, the quality of visual content is crucial, especially in the field of sports, and the development of IR technology is of significant significance to enhance the audience experience and the accuracy of professional analysis. Facing the common fuzzy and noise problems in FVI, the study designs a GECM algorithm based on the FCM algorithm by integrating the advantages of fuzzy logic and cluster analysis and introducing the generalized equilibrium theory to effectively deal with MB and background noise. The results revealed that the average running time of the GECM algorithm on the ImageNet dataset is 2.45 seconds, which shows a significant speed advantage compared to the 7.73 seconds of the traditional FCM algorithm and the 12.41 seconds of the BF. In terms of edge information retention, the GECM algorithm achieved a low rate of image edge information loss, with a negligible error from the actual image edge information loss rate, proving the algorithm's high accuracy and fidelity in preserving details. In terms of peak SNR and structural similarity, the GECM algorithm achieved a peak SNR of 28.23 and a structural similarity of 0.915 on the Cameraman test image, which also demonstrated better performance than the traditional method. The above results indicate that the GECM algorithm has demonstrated its efficient processing speed and good detail preservation ability in football video image restoration, and its restored image quality is high. However, in practical application scenarios, due to the complexity and variability of the environment, the complexity of the noise model and the degree of motion blur may exceed the processing range of the current algorithm. Therefore, future research will further optimize the algorithm to enhance its adaptive ability. And develop more intelligent noise processing techniques and combine algorithms with other advanced deep learning methods to adapt to different types of noise and complex dynamic scenes, thereby improving the robustness of the algorithm.

Competing Interests

The authors have any competing interests in the manuscript.

Data Availability Statement

Data will be made available on reasonable request.

Reference

[1] Sadok I, Masmoudi A, Zribi M. Integrating the EM algorithm with particle filter for image restoration with exponential dispersion noise. Communications in Statistics-Theory and Methods, 2023, 52(2): 446-462.

[2] Mei Y, Fan Y, Zhang Y, Yu J, Zhou Y, Liu D, Shi H. Pyramid attention network for image restoration. International Journal of Computer Vision, 2023, 131(12): 3207-3225.

[3] Luo N, Yu H, You Z, Li Y, Zhou T, Jiao Y, Qiao S. Fuzzy logic and neural network-based risk assessment model for import and export enterprises: A review. Journal of Data Science and Intelligent Systems, 2023, 1(1): 2-11.

[4] Zhang X, Cui J, Jia Y, Zhang P, Song F, Cao X, Zhang G. Image restoration for blurry optical images caused by photon diffusion with deep learning. JOSA A, 2023, 40(1): 96-107.

[5] Maulana Akbar J, Ignatius Moses Setiadi D R. Joint method using Akamatsu and discrete wavelet transform for image restoration. Applied computing and informatics, 2023, 19(3/4): 226-238.

[6] Hasanvand M, Nooshyar M, Moharamkhani E, Selyari A. Machine Learning Methodology for Identifying Vehicles Using Image Processing//Artificial Intelligence and Applications. 2023, 1(3): 170-178.

[7] Sharma P, Bisht I, Sur A. Wavelength-based attributed deep neural network for underwater image restoration. ACM Transactions on Multimedia Computing, Communications and Applications, 2023, 19(1): 1-23.

[8] Zhang K, Li Y, Zuo W, Zhang L, Van Gool L, Timofte R. Plug-and-play image restoration with deep denoiser prior. IEEE Transactions on Pattern Analysis and Machine Intelligence, 2021, 44(10): 6360-6376.

[9] Pan J, Dong J, Liu Y, Zhang J, Ren J, Tang J, Yang M H. Physics-based generative adversarial models for image restoration and beyond. IEEE transactions on pattern analysis and machine intelligence, 2020, 43(7): 2449-2462.

[10] Zha Z, Wen B, Yuan X, Zhou J, Zhu C, Kot A C. A hybrid structural sparsification error model for image restoration. IEEE Transactions on Neural Networks and Learning Systems, 2021, 33(9): 4451-4465.

[11] Mei Y, Fan Y, Zhang Y, Yu J, Zhou Y, Liu D, Shi H. Pyramid attention network for image restoration. International Journal of Computer Vision, 2023, 131(12): 3207-3225.

[12] He W, Yao Q, Li C, Yokoya N, Zhao Q, Zhang H, Zhang L. Non-local meets global: An iterative paradigm for hyperspectral image restoration. IEEE Transactions on Pattern Analysis and Machine Intelligence, 2020, 44(4): 2089-2107.

[13] Hu B, Li L, Liu H, Lin W, Qian J. Pairwise-comparison-based rank learning for benchmarking image restoration algorithms. IEEE Transactions on Multimedia, 2019, 21(8): 2042-2056.

[14] Jiu M, Pustelnik N. A deep primal-dual proximal network for image restoration. IEEE Journal of Selected Topics in Signal Processing, 2021, 15(2): 190-203.

[15] Chen Y, He W, Yokoya N, Huang T Z. Hyperspectral image restoration using weighted group sparsity-regularized low-rank tensor decomposition. IEEE transactions on cybernetics, 2019, 50(8): 3556-3570.

[16] Yu K, Wang X, Dong C, Tang X, Loy C C. Path-restore: Learning network path selection for image restoration. IEEE Transactions on Pattern Analysis and Machine Intelligence, 2021, 44(10): 7078-7092.

[17] Zamir S W, Arora A, Khan S, Hayat M, Khan F S, Yang M H, Shao L. Learning enriched features for fast image restoration and enhancement. IEEE transactions on pattern analysis and machine intelligence, 2022, 45(2): 1934-1948.

[18] Jin Z, Iqbal M Z, Bobkov D, Zou W, Li X, Steinbach E. A flexible deep CNN framework for image restoration. IEEE Transactions on Multimedia, 2019, 22(4): 1055-1068.

[19] Fu B, Dong Y, Fu S, Wu Y, Ren Y, Thanh D N. Multistage supervised contrastive learning for hybrid-degraded image restoration. Signal, Image and Video Processing, 2023, 17(2): 573-581.

[20] Zhang J, Pan D, Zhang K, Jing J, Ma Y, Chen M. Underwater single-image restoration based on modified generative adversarial net. Signal, Image and Video Processing, 2023, 17(4): 1153-1160.

[21] Chen Y, Xia R, Zou K, Yang K. RNON: image inpainting via repair network and optimization network. International Journal of Machine Learning and Cybernetics, 2023, 14(9): 2945-2961.

[22] Wang W, Li F, Ng M K. Structural similarity-based nonlocal variational models for image restoration. IEEE Transactions on Image Processing, 2019, 28(9): 4260-4272.

[23] Hasanvand M, Nooshyar M, Moharamkhani E, Selyari A. Machine Learning Methodology for Identifying Vehicles Using Image Processing//Artificial Intelligence and Applications. 2023, 1(3): 170-178.

[24] Pham C T, Tran T H I T H U T, Dang H V I, Dang H P. An adaptive image restoration algorithm based on hybrid total variation regularization. Turkish Journal of Electrical Engineering and Computer Sciences, 2023, 31(1): 1-16.

[25] Zhang Z, Huang Y, Bao S, Liu Z. Panoramic annular image restoration algorithm by prediction based on the lens design characteristics. Applied Optics, 2023, 62(3): 518-527.

[26] Neole B. Application of Mathematical Modelling and Deep Learning in Image Restoration using Edge Preservation Method. Communications on Applied Nonlinear Analysis, 2024, 31(2): 496-514.

[27] Chen Y, Xia R, Yang K, Zou K. GCAM: lightweight image inpainting via group convolution and attention mechanism. International Journal of Machine Learning and Cybernetics, 2024, 15(5): 1815-1825.

[28] Li L, Liu X, Shi F, Cai Y, Zhang Y, Fang P, Weng N. Foggy image restoration using deep sub-pixel reconstruction network. IET Image Processing, 2024, 18(3): 707-721.